Communication

# Mapping Chemical Exchange in Proteins with MW > 50 kD

Chunyu Wang, Mark Rance, and Arthur G. Palmer

*J. Am. Chem. Soc.*, **2003**, 125 (30), 8968-8969• DOI: 10.1021/ja035139z • Publication Date (Web): 04 July 2003



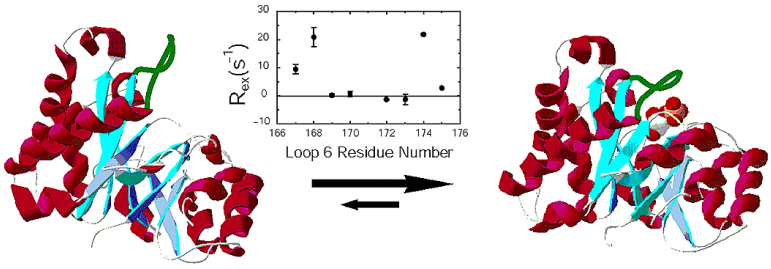


## More About This Article

Additional resources and features associated with this article are available within the HTML version:

- Supporting Information
- Links to the 4 articles that cite this article, as of the time of this article download
- Access to high resolution figures
- Links to articles and content related to this article
- Copyright permission to reproduce figures and/or text from this article

View the Full Text HTML

J|A|C|S
COMMUNICATIONS

Published on Web 07/04/2003

# Mapping Chemical Exchange in Proteins with MW > 50 kD

Chunyu Wang,[†] Mark Rance,[‡] and Arthur G. Palmer, III*,[†]

*Department of Biochemistry and Molecular Biophysics, Columbia University, 630 West 168th Street, New York, New York 10032, and Department of Molecular Genetics, Biochemistry and Microbiology, University of Cincinnati College of Medicine, 231 Albert Sabin Way, Cincinnati, Ohio 45267-0524*

Received March 13, 2003; E-mail: agp6@columbia.edu

Chemical exchange phenomena in nuclear magnetic resonance (NMR) spectroscopy of proteins in solution arise from motions on $\mu$s to ms time scales that can be critical for ligand binding,[1] catalysis,[2] and allosteric regulation.[3] Use of chemical exchange to study these biological processes usually has been restricted to proteins with molecular weight (MW) < 25 kD.[4] The chemical exchange contribution to transverse relaxation, $R_{ex}$, is independent of protein size and consequently is a smaller fraction of the apparent transverse relaxation rate constant, $R_2$, for larger proteins. In addition, NMR spectroscopy of larger proteins is hindered by severe resonance overlap and rapid transverse relaxation. This Communication describes a novel experiment for rapid identification of chemical exchange in $^2$H/$^{15}$N-labeled proteins with MW ranging from 15 to >50 kD. The technique is demonstrated in *Escherichia coli* ribonuclease H (RNaseH), a monomer with MW = 17 kD, and *Saccharomyces cerevisiae* triosephosphate isomerase (TIM), a symmetric dimer with total MW = 54 kD.

Interference between $^1$H−$^{15}$N dipole−dipole (DD) and $^{15}$N chemical shift anisotropy (CSA) interactions results in different relaxation rate constants and line width for the two components of the scalar-coupled amide $^{15}$N doublet. The transverse relaxation rate constants, $R_2^{\alpha}$ and $R_2^{\beta}$, for the narrow (corresponding to the H$^{\alpha}$N$^-$ transition) and broad (corresponding to the H$^{\beta}$N$^-$ transition) doublet components, respectively, are given by:[5,6]

$$R_2^{\alpha} = R_2^0 - \eta_{xy} + R_1^{H}/2 + R_{ex}$$
$$R_2^{\beta} = R_2^{\alpha} + 2\eta_{xy} \quad (1)$$

where $R_2^0$ is the auto-relaxation rate constant for in-phase $^{15}$N magnetization from $^{15}$N CSA and $^1$H−$^{15}$N DD interactions, $\eta_{xy}$ is the rate constant for cross-correlation between $^{15}$N CSA and $^1$H−$^{15}$N DD interactions, and $R_1^H$ is the longitudinal relaxation rate for the $^1$H$^N$ spin from CSA and DD interactions with remote $^1$H spins. For $^2$H/$^{15}$N-labeled proteins at high magnetic fields, $R_2^{\alpha} \ll R_2 = R_2^0 + R_{ex}$ which facilitates the detection of $R_{ex}$. Although $R_2^0$ cannot be directly measured for exchanging sites, $\kappa = R_2^0/\eta_{xy}$ is independent of chemical exchange, local motions or global dynamics in large proteins.[7,8] Thus, $R_{ex}$ is determined by:

$$R_{ex} = R_2^{\alpha} - R_1^{2HzNz}/2 - \eta_{xy}(\kappa - 1) + R_1^{N}/2 \quad (2)$$

in which $R_1^{2HzNz} \approx R_1^H + R_1^N$ is the relaxation rate constant for longitudinal two-spin order and $R_1^N$ is the longitudinal relaxation rate of the $^{15}$N spin. Values of $\kappa$ are derived from the trimmed mean of $1 + (R_2^{\alpha} - R_1^{2HzNz}/2)/\eta_{xy}$,[9] or theoretical calculations.[7,8] $R_1^N$ is small and can be neglected in eq 2 for proteins with MW > 30 kD (e.g., $\langle R_1^N \rangle = 0.44 \pm 0.04$ s$^{-1}$ in TIM); for smaller proteins, $R_1^N$ can be measured using conventional experiments.[10]

[†] Columbia University.
[‡] University of Cincinnati.

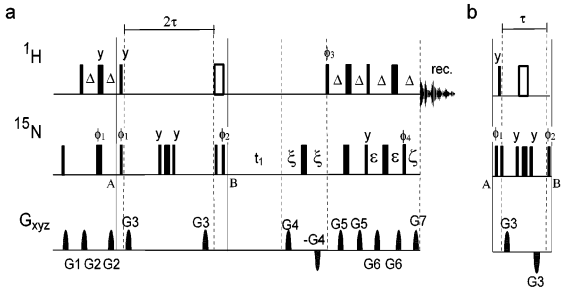


***Figure 1.*** Pulse sequences for measuring $R_2^{\alpha}$, $R_2^{\beta}$, and $R_1^{2HzNz}$ to detect chemical exchange in large proteins. The sequence shown in (a) detects relaxation of the narrow doublet component during the Hahn echo period $2\tau$ when the proton composite pulse element (open bar) is $(90°_x 90°_y 90°_{-y} 90°_{-x})$ and detects relaxation of the broad doublet component when this element is $(90°_x 90°_y 90°_y 90°_x)$. Relaxation of longitudinal two-spin order is detected if the sequence between points A and B in (a) is replaced with (b); the proton composite pulse is $(90°_x 90°_y 90°_y 90°_x)$. Composite pulses are applied at the center of amide $^1$H. Narrow and wide solid bars are 90° and 180° pulses, respectively. All pulses have *x* phase unless otherwise stated. Phase cycles are $\phi_1 = x, -x$; $\phi_2 = x, x, -x, -x$; $\phi_3 = y$; $\phi_4 = x$; and receiver phase $= -x, x, x, -x$. Gradients G4 and G7 are used for coherence selection; other gradients are for artifact suppression. Echo−antiecho quadrature detection is achieved by inverting $\phi_3$, $\phi_4$, and the sign of gradient G4;[12] axial peaks are shifted by inverting $\phi_1$, and the receiver phase. Other delays are $\Delta = 2.7$ ms, $\xi = 950$ $\mu$s, $\epsilon = 2.675$ ms, $\zeta = 250$ $\mu$s.

Pulse sequences for measuring $R_2^{\alpha}$, $\eta_{xy}$, and $R_1^{2HzNz}$ in large proteins are shown in Figure 1. During the Hahn echo period of length $2\tau$ in Figure 1a, the narrow and broad doublet components relax independently because cross relaxation between the doublet components is suppressed when $2\tau = N/J_{NH}$ and $2\pi J_{NH} \gg R_1^H/2$, in which $N$ is an integer and $J_{NH}$ is the scalar coupling constant.[11] The α and $\beta$ spin states of $^1$H spins are interchanged by a 180° proton pulse. Therefore, if the proton composite pulse element in Figure 1a is effectively a 0° or 180° pulse (see Figure 1 caption for details), the intensity of the narrow or broad doublet component is recorded by the TROSY scheme following point B, respectively. Figure 1b shows modifications of Figure 1a necessary to measure $R_1^{2HzNz}$ during a relaxation period $\tau$.

The intensity decays for the three experiments are given by:

$$I^{\alpha}(2\tau) = I(0)\exp[-2\tau R_2^{\alpha}] \quad (3)$$

$$I^{\beta}(2\tau) = I(0)\exp[-2\tau R_2^{\beta}] \quad (4)$$

$$I^{2HzNz}(\tau) = I(0)\exp[-\tau R_1^{2HzNz}] \quad (5)$$

in which the prefactor $I(0)$ is the same in eqs 3−5 because the three pulse sequences have identical delays and number of pulses when $\tau = 0$. Thus, the rate constants needed to determine $R_{ex}$ using


10.1021/ja035139z CCC: $25.00 

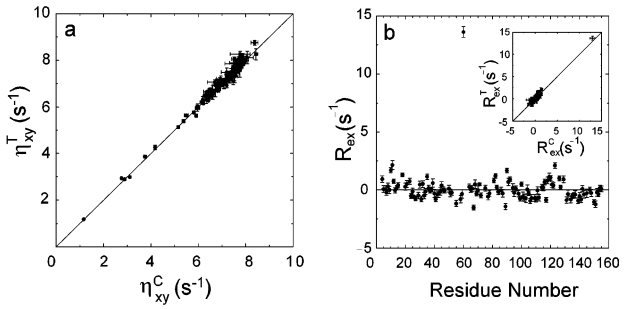


***Figure 2.*** Measurements of (a) $\eta_{xy}$ and (b) $R_{ex}$ for [85%-D, U-$^{15}$N] *E. coli* RNaseH using the pulse sequences in Figure 1. Values of $\eta_{xy}$ obtained from the pulse sequence depicted in Figure 1a, denoted as $\eta_{xy}^T$, are plotted versus values measured from conventional sequences, denoted as $\eta_{xy}^C$. The inset of Figure 2b compares the $R_{ex}$ obtained from conventional $R_2$ and $\eta_{xy}$ measurements ($R_{ex}^c$) and from the new sequences ($R_{ex}^T$). The relaxation delay $2\tau = 10/J_{NH} = 108$ ms, corresponding to $I^\beta(2\tau)/I^\alpha(2\tau) = 0.3$ for most residues. $\kappa$ was determined by the trimmed mean of $1 + (R_2^\alpha - R_1^{2HzNz}/2 + R_1^N/2)/\eta_{xy}$ to be 1.4. For nonexchanging residues, $R_{ex}$ is distributed around zero with a standard deviation of 0.6 s$^{-1}$ due to variation in magnitude and orientation of the $^{15}$N CSA tensor.[8] Data were collected in triplicate with a 1.0 mM sample at 310 K on a Bruker DRX600 spectrometer equipped with a triple resonance probe.

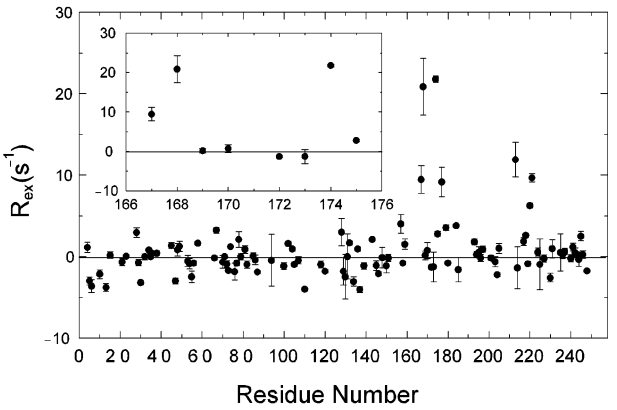


***Figure 3.*** Chemical exchange in G3P bound [85%-D, U-$^{15}$N] TIM detected using the pulse sequences in Figure 1. The insert is an expanded view of the region encompassing residues in the active site loop 6. The relaxation delay $2\tau = 2/J_{NH} = 21.6$ ms, corresponding to $I^\beta(2\tau)/I^\alpha(2\tau) = 0.3$ for most residues. $\kappa$ was determined by the trimmed mean of $1 + (R_2^\alpha - R_1^{2HzNz}/2)/\eta_{xy}$ to be 1.2. For nonexchanging residues, $R_{ex}$ is distributed around zero with a standard deviation of 1.7 s$^{-1}$ due to variation in magnitude and orientation of the $^{15}$N CSA tensor.[8] The data were collected in quadruplicate on a 1 mM TIM (with 10 mM G3P) sample at 800 MHz using a Bruker DRX800 NMR spectrometer equipped with a triple-resonance cryoprobe.

eq 2 are obtained from the intensity ratios:

$$I^\beta(2\tau)/I^\alpha(2\tau) = \exp[-4\tau\eta_{xy}] \quad (6)$$

$$I^\alpha(2\tau)/I^{2HzNz}(\tau) = \exp[-2\tau(R_2^\alpha - R_1^{2HzNz}/2)] \quad (7)$$

The rate constants are determined by curve-fitting the intensity ratios measured at different values of $\tau$, or by repeatedly measuring duplicate spectra with a single value of $\tau$.[13]

The new experiments incorporate a number of features to improve sensitivity and accuracy for larger proteins. First, TROSY (transverse relaxation optimized spectroscopy) is employed during the $t_1$ evolution and $t_2$ detection periods for improved resolution and sensitivity in large proteins.[5] $R_2^\alpha$ and $R_2^\beta$ are measured independently to obtain $\eta_{xy}$, because independent detection of in-phase and anti-phase $^{15}$N magnetization, as used in conventional experiments for measuring $\eta_{xy}$,[7,14] is difficult to utilize with TROSY. Second, $^1$H 180° pulses or composite pulse sequences are not used for decoupling during the Hahn echo period. Decoupling can interfere with echo formation and increase apparent relaxation rate constants.[11] Third, data are not recorded for $\tau = 0$; therefore, a minimum of three 2D spectra are sufficient to determine $R_{ex}$ using eqs 2, 6, and 7. Fourth, the uncertainty in $R_{ex}$ contributed by the $\eta_{xy}$ measurement is scaled down by a factor of $\kappa/(\kappa - 1)$, which is more than 6-fold at 800 MHz, compared with approaches that obtain $R_{ex} = R_2 - \kappa\eta_{xy}$ from $R_2$ and $\eta_{xy}$.[9] As in all experiments involving anti-phase $^{15}$N magnetization, the sensitivity of these sequences may be reduced for solvent-exposed residues by rapid amide proton exchange, especially at high pH.

The proposed technique was validated using RNaseH. As shown in Figure 2, good agreement is obtained between $\eta_{xy}$ and $R_{ex}$ obtained from the new and conventional pulse sequences.[7] Chemical exchange is detected for residues Lys60 and Trp90, in agreement with previous reports.[7] Small exchange contributions are also evident for residues near positions 10 and 120.

The new methods were applied to glycerol 3-phosphate (G3P) bound TIM to illustrate the advantages for larger proteins. In TIM, the average $^{15}$N $R_2$ is 37 s$^{-1}$ at 800 MHz at 298 K, while the average $R_2^\alpha$ is only 6 s$^{-1}$. Therefore, the relative contribution of $R_{ex}$ to $R_2^\alpha$ can be 6 times as high as the contribution to $R_2$. As shown in Figure 3, chemical exchange broadening caused by the well-known loop motion in TIM[15] is observed for residues at the N (residues V167 and W168) and C termini (residues L174) hinge of loop 6. Other residues (T177, N213, F220, and K221) with significant chemical exchange are located in the vicinity of loop 6 in the 3D structure of TIM. These results are consistent with the hypothesis that the termini of the loop act as the hinges.[15]

The techniques presented herein allow detection of conformational exchange processes in proteins with MW > 50 kD. Thus, these methods, along with the TROSY-CPMG experiment,[16,17] expand the capacity of NMR spectroscopy to investigate $\mu$s−ms time scale motions involved in protein function.

**Acknowledgment.** We thank Joel Butterwick for providing the *E. coli* RNaseH sample. This work was supported by NIH Grants DK07328 (C.W.), GM40089 (M.R.), and GM59273 (A.G.P.). A.G.P. is a member of the New York Structural Biology Center supported by NIH Grant GM66354.

**References**

(1) Mulder, F. A.; Mittermaier, A.; Hon, B.; Dahlquist, F. W.; Kay, L. E. *Nat. Struct. Biol.* **2001**, *8*, 932−935.
(2) Eisenmesser, E. Z.; Bosco, D. A.; Akke, M.; Kern, D. *Science* **2002**, *295*, 1520−1523.
(3) Volkman, B. F.; Lipson, D.; Wemmer, D. E.; Kern, D. *Science* **2001**, *291*, 2429−2433.
(4) Palmer, A. G.; Kroenke, C. D.; Loria, J. P. *Methods Enzymol.* **2001**, *339*, 204−238.
(5) Pervushin, K.; Riek, R.; Wider, G.; Wüthrich, K. *Proc. Natl. Acad. Sci. U.S.A.* **1997**, *94*, 12366−12371.
(6) Goldman, M. *J. Magn. Reson.* **1984**, *60*, 437.
(7) Kroenke, C. D.; Loria, J. P.; Lee, L. K.; Rance, M.; Palmer, A. G. *J. Am. Chem. Soc.* **1998**, *120*, 7905−7915.
(8) Fushman, D.; Tjandra, D.; Cowburn, D. *J. Am. Chem. Soc.* **1998**, *120*, 10947−10952.
(9) Wang, C.; Grey, M. J.; Palmer, A. G. *J. Biomol. NMR* **2001**, *21*, 361−366.
(10) Farrow, N. A.; Muhandiram, R.; Singer, A. U.; Pascal, S. M.; Kay, C. M.; Gish, G.; Shoelson, S. E.; Pawson, T.; Forman-Kay, J. D.; Kay, L. E. *Biochemistry* **1994**, *33*, 5984−6003.
(11) Palmer, A. G.; Skelton, N. J.; Chazin, W. J.; Wright, P. E.; Rance, M. *Mol. Phys.* **1992**, *75*, 699−711.
(12) Weigelt, J. *J. Am. Chem. Soc.* **1998**, *120*, 10778−10779.
(13) Jones, J. A. *J. Magn. Reson.* **1997**, *126*, 283−286.
(14) Tjandra, N.; Szabo, A.; Bax, A. *J. Am. Chem. Soc.* **1996**, *118*, 6986−6991.
(15) Joseph, D.; Petsko, G. A.; Karplus, M. *Science* **1990**, *249*, 1425−1428.
(16) Loria, J. P.; Rance, M.; Palmer, A. G. *J. Biomol. NMR* **1999**, *15*, 151−155.
(17) Yuan, Y.; Simplaceanu, V.; Lukin, J. A.; Ho, C. *J. Mol. Biol.* **2002**, *321*, 863−878.

JA035139Z